Nitrogen-mediated interaction in polyacrylamide–silver nanocomposites

2006 J. Phys.: Condens. Matter 18 11233

(http://iopscience.iop.org/0953-8984/18/49/015)

INSTITUTE OF PHYSICS PUBLISHING JOURNAL OF PHYSICS: CONDENSED MATTER

J. Phys.: Condens. Matter **18** (2006) 11233–11242 doi:10.1088/0953-8984/18/49/015

Nitrogen-mediated interaction in polyacrylamide–silver nanocomposites

S Mukherjee and M Mukherjee

Surface Physics Division, Saha Institute of Nuclear Physics, 1/AF, Bidhannagar, Kolkata-700064, India

Received 3 August 2006, in final form 11 October 2006
Published 22 November 2006
Online at stacks.iop.org/JPhysCM/18/11233

Abstract

Polyacrylamide (PAM)–silver nanocomposite materials have been synthesized by the reduction of the silver salt in the polyacrylamide matrix. Silver nanoparticles embedded in the polymer matrix, observed through transmission electron microscopy (TEM), suggests attractive polymer–particle interaction. Detailed spectroscopic investigations have been carried out on the nanocomposite samples using a range of techniques to understand the nature of the interaction. The x-ray photoelectron spectroscopy (XPS) core level spectra and Fourier-transform infrared (FTIR) spectroscopy results indicate that the nanoparticles are attached to the pendant group of the polymer through physical interactions. The XPS valence band study confirms that the interaction between the polymer and the silver nanoparticles occurs through partial charge transfer from the metal particles to the nitrogen sites of the polymer side chains. The modifications associated with the silver nanoparticles are mainly due to confinement effects.

(Some figures in this article are in colour only in the electronic version)

1. Introduction

Silver is one of the most widely used noble metals that finds applications in its colloidal or nanocrystalline form in many physical applications, such as in the form of dopant in a dielectric medium for the enhancement of optical properties [1] or in biological applications where the use of colloidal silver for medicinal purposes is an age-old practice [2–4]. Polymer-coated functionalized noble metal nanoparticles have recently emerged as an active field of research [5–11] due to many novel properties of these materials. A growing interest has been developed in water-soluble polymers for their various application potentials in physical and biological systems [12–15]. These polymers may also be considered as a model system for their biological counterparts such as proteins and may be used to study their adhesion properties through physical or chemical interaction with nanocrystalline metal particles. It has been realized that the interaction between the particles and the host matrix plays a crucial

role in determining the structural and dynamical behaviours of the composite systems. It is of further significance to have knowledge about the nature of the interaction and the exact interacting sites of the host in order to have control over their synthesis and applications. Although water-soluble polymers are hydrophilic in nature and the clean metal surfaces are normally hydrophobic, they have been used as a medium to grow silver nanoparticles very successfully [16, 17]. In the present study, we have grown nanocrystalline metallic silver particles in a water-soluble polymer medium by a chemical reduction technique. We have performed various microscopic and spectroscopic studies to understand the exact nature of polymer–metal interaction in this system. We find that the interactions between the polymer and the nanoparticles are physical or weakly chemical in nature and are mediated through the nitrogen sites of the polymer molecules.

2. Experimental details

Silver–polyacrylamide nanocomposites having two widely different volume fractions of silver in polyacrylamide were prepared using the following method [17]. For the first sample (sample I), 8 mg of $AgNO_3$ was dissolved in distilled water (Millipore Milli-Q, $\rho = 18.2$ MΩ cm) and NaOH was added, resulting in a brown precipitate of Ag_2O. The precipitate was washed with distilled water and dissolved in dilute ammonia solution. The silver–ammonia complex thus formed was added to polyacrylamide (Polysciences Inc., USA, $M_w = 5 \times 10^6$) solution (10 mg ml^{-1}) and the initial volume of the solution was made up to 500 ml by adding water. The solution was stirred with a magnetic stirrer, with simultaneous purging by dry N_2 gas for 5 min, and thereafter 5 ml of 40% formic acid was added to it as reducing agent. The colourless solution was then stirred again and boiled until the final volume was reduced to 20 ml and the solution developed a yellow colour. Excess formic acid was then added to the solution for the complete reduction of the silver complex. A blackish yellow colour was observed at this stage. The requirement of higher temperature and excess amount of formic acid shows that the reduction procedure was slowed down by the presence of the polymer. This indicates that the polymer only provides a weak oxidizing environment and plays no direct role in the reduction process. For the other sample (sample II), 15 mg of $AgNO_3$ was taken as the starting material and the above procedure was followed. After boiling and reducing the volume of solution to 20 ml, the light-yellow coloured material sticking to the walls of the container was collected and redissolved in water. It is important to note that the preparation of the silver–ammonia complex is also possible by directly adding a suitable amount of ammonia in the initial silver nitrate solution, which may result in nitrates in the final material. The present procedure of intermediate oxide stage was adopted to avoid the presence of nitrates.

Although the initial silver concentration for sample II was more than that of sample I the procedure of collection of the material from the wall of the container (instead of the entire sol, as was the case for sample I) gives rise to a much lower silver volume fraction in sample II with similar average particle size in both the samples. It was observed that the solubility of the dried nanocomposite materials was greatly reduced as compared to that of the pure polymer as a result of polymer–particle attachment. The samples were characterized using dynamic light scattering (DLS), TEM, UV–visible (UV–vis), FTIR and XPS techniques. The DLS of the dilute solutions (0.25 mg ml^{-1}) of the pure PAM and the nanocomposites were performed using a Malvern zetasizer nano-s spectrometer. For TEM microstructural studies a drop of the composite sol was taken on a carbon-coated copper grid which was then dried at room temperature. The electron microscopy studies were done on the samples with a JEOL JEM-2010 microscope operated at 200 kV. The UV–vis spectra of the composite sols were taken with a GBC Cintra 10e spectrometer. FTIR spectra of free-standing films of the samples

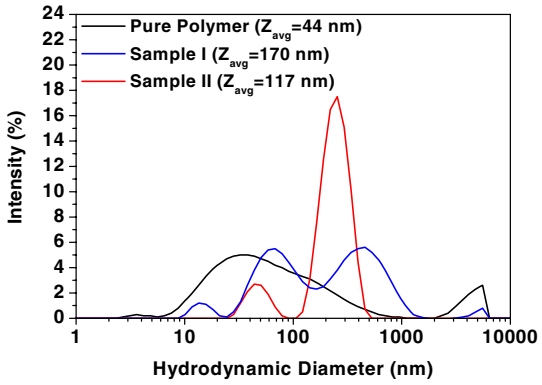

Figure 1. Hydrodynamic diameter distribution observed from DLS for the pure polymer and the nanocomposite samples. Average diameters Z_{avg} for the samples are indicated in the figure.

were taken in transmission mode with a PerkinElmer Spectrum GX system. Films for XPS study were prepared by drop casting on a clean silicon substrate placed in a Teflon sample tray and were dried in an oven at 90 °C for a week. The nominal thicknesses of the films used for XPS study were 10 μm. XPS core-level and valence-band spectra were taken with an Omicron Multiprobe (Omicron NanoTechnology GmbH, UK) spectrometer fitted with an EA125 hemispherical analyser. A low-energy electron gun (SL1000, Omicron) with a large spot size was used to neutralize the sample. The potential of the electron gun was kept fixed at -3 eV with respect to the ground. A monochromated Al Kα x-ray source operated at 150 W was used for the experiments. The analyser pass energy was kept fixed at 20 eV for all the scans.

3. Results and discussion

Dynamic light scattering that measures the statistically averaged size of the polymer coils in solutions was used to measure the hydrodynamic radius R_{H} of the polymer and the nanocomposite coils in dilute solutions. In this method the Stokes–Einstein equation $R_{\mathrm{H}} = \frac{k_{\mathrm{B}}T}{6\pi\,\eta\,D}$ is used to obtain R_{H} in terms of the diffusion coefficient D of the Brownian motion of the individual polymer (or composite) coils in the solution and coefficient of viscosity η of the solvent. In figure 1 we have shown the hydrodynamic diameter distribution of the nanocomposite sols along with the pure PAM. A comparison of the data shows that the size distributions of the nanocomposite sols have altered dramatically due to the attachment of the silver particles. For the nanocomposite samples the average size of the polymer chains (with silver particles attached) are found to be much larger. Narrower peaks in the case of composites as compared to a broad distribution for the pure polymer have also been observed as a result of polymer–particle interaction. The differences in the DLS data between the two nanocomposites are due to the difference in the sample preparation.

In figure 2(a), a representative micrograph of the composite material (sample I) is shown. The corresponding size distribution of the nanocrystalline particles is shown in figure 2(b). It can be clearly observed from the figure that the individual particles are embedded in the polymer matrix in the form of agglomerates. It was interesting to note that the average size of these units was very close to those observed from DLS, indicating that the nanocomposite material is composed of such polymer-encapsulated silver nanoparticles resulting from mutual attractive interaction.

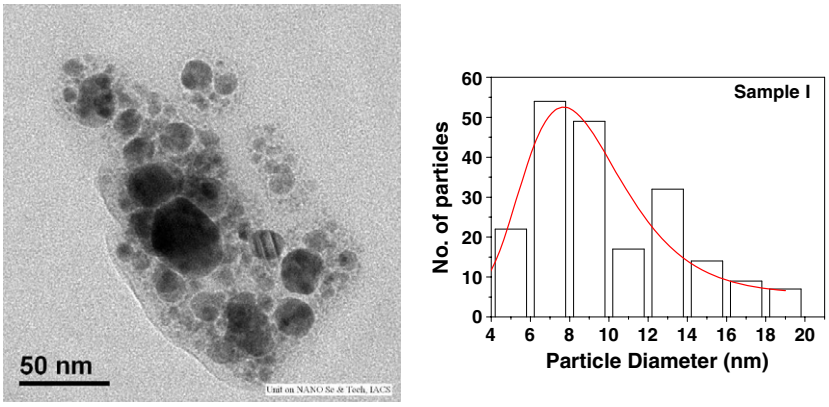

(a) **(b)**

Figure 2. (a) Transmission electron micrograph of sample I. (b) Size distribution of the silver nanoparticles for the sample. A theoretical fit to a log-normal distribution has been shown with a continuous line in (b). The average particle diameters and geometric standard deviations obtained from the fits are 9 nm and 1.4 respectively.

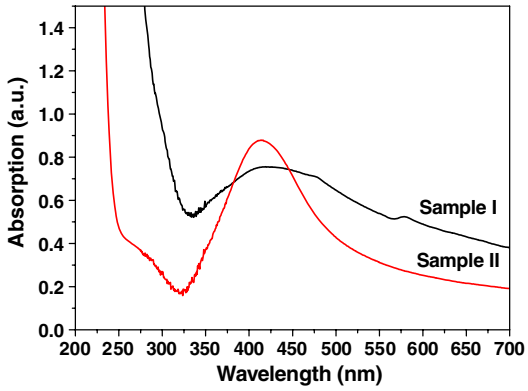

Figure 3. UV–visible absorption spectra of Ag nanoparticles in polyacrylamide. The curves have been suitably normalized for clarity.

The optical absorption behaviour for the nanocomposite samples I and II are shown in figure 3. As is seen from the figure, the surface plasmon peak for sample II occurs at 412 nm, which is typical for small Ag particles embedded in a dielectric medium [1, 18–20]. For sample I the peak is red-shifted and appears at 420 nm. It has already been observed that with increased aggregation of particles the plasmon absorption peak shifts to higher wavelength [21, 22]. In the case of sample I the amount of aggregation is likely to be more compared to that of sample II due to the higher silver concentration in the former. Broadening of the absorption peak for sample I may be attributed to the longitudinal plasmon peaks [22, 23] appearing around 475 and 575 nm due to the higher amount of aggregation and formation of chainlike structures in this sample. Such chainlike structures have also been observed in TEM micrographs (not shown).

FTIR spectroscopy is one of the most sensitive tools for observing the interaction between the polymer molecules and the nanoparticles through the modifications in the vibrational

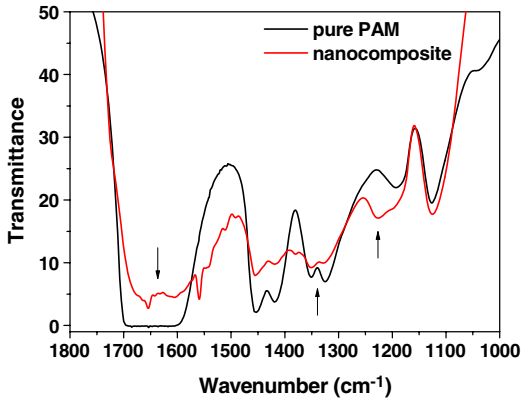

Figure 4. FTIR spectra of nanocomposite (sample I) compared with pure polyacrylamide. The modified regions are indicated by arrows.

spectra. In figure 4 we have compared the important region of the FTIR transmission spectra for sample I with that of pure polyacrylamide. The deviations in the spectra were found to occur only in the region 1700–1100 cm^{-1}. Three significant observations in the data are (i) the modification of the band near 1650 cm^{-1}, (ii) the modification of intensity ratio of the two peaks near 1350 cm^{-1} and (iii) the appearance of a new absorption band near 1250 cm^{-1}. In the linear chain polyacrylamide, the functional amide group ($–CONH_2$) is attached to the saturated C–C backbone. It is likely that the silver particles attach to the polymer chains through the functional (amide) groups. For the pure polymer the absorption band due to NH_2 bending appears near 1655–1620 cm^{-1}. The amide II band which results from the interaction between N–H bending and C–N stretching of the C–N–H group lies in the region of 1570–1515 cm^{-1}. These characteristic bands lie under the envelope of the strong C=O stretching band for the system. The C–N stretching band for the polymer occurs near 1400 cm^{-1}. A weaker band near 1250 cm^{-1} results from interaction between the N–H bending and C–N stretching vibrations [24, 25]. In the present nanocomposite the observed broadening and red-shift of the peak near 1650 cm^{-1}, arising out of C=O stretching, NH_2 bending and the coupling modes between C–N stretching and N–H bending, is due to the interaction between the amide group and the silver nanoparticles. The alteration of intensity ratio of the two peaks near 1350 cm^{-1} may be attributed to the modifications in the C–N stretching modes. The advent of a new band near 1250 cm^{-1} also suggests significant changes in the interactions between N–H bending and C–N stretching modes. The alteration of the vibrational spectra of the nanocomposite material indicates that the C–N and N–H modes are mainly affected by the polymer–particle interaction. However, the modifications in C=O stretching modes cannot be completely ruled out considering its overlapping position.

It is clear from the FTIR study that the silver particles are attached to the polymer through the side chains, but the important questions are what the nature of interaction is and which atoms are involved in the process. For the chemical analysis of the materials and in order to identify the nature and specific sites of interaction in the nanocomposites we have performed XPS core level and valence band studies of all the samples. For quantitative analysis, the background arising in the data due to the secondary electrons was corrected using the Shirley method [26]. The silver to nitrogen atomic ratios obtained from core level XPS for samples I and II were 1:5.6 and 1:36.6 respectively, showing the wide variation in the silver concentration between the two samples. The survey scans for the pure PAM and sample I are shown in

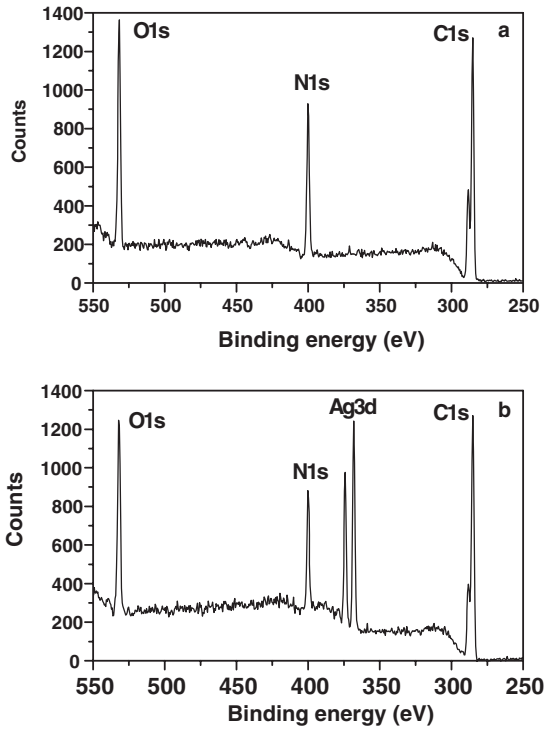

Figure 5. XPS survey spectra of (a) pure polymer and (b) nanocomposite (sample I). All peak positions were normalized with respect to the major peak in the C 1s spectra at 285.2 eV.

figure 5 for comparison. The binding energies for the O 1s, N 1s and C 1s levels for the nanocomposite samples were observed to be unaltered when compared to the pure polymer; however, the intensities of the O 1s and N 1s lines were found to be reduced in the case of the nanocomposite, indicating that these atoms are more populated at the polymer–metal interface and are shadowed by the outer polymer layers. No shifts in the core level energies in XPS spectra are interpreted as the polymer–particle interaction acts as a weak perturbation to the polymeric system. The Ag $3d_{5/2}$ lines, as shown in figure 6(a), at the positions 368.1 eV (sample I) and 368.5 eV (sample II), are shifted from the position for bulk Ag (368.0 eV) along with a systematic increase of peak widths. It was observed earlier that for non-interacting nanosized metallic particles the core levels are shifted to the higher binding energies [27, 28]. We attributed the present change of the silver binding energy to the quantum size effect of the non-interacting (or weakly interacting) silver particles [28]. The C 1s level for the nanocomposite materials along with that of the pure polymer are shown in figure 6(b). In PAM there are three carbon environments [29] (two for the backbone chain and one for the pendant $–CONH_2$ group). Since the peak positions corresponding to the two backbone carbon atoms are very close and are separated by about 3 eV from that of the pendant carbon atom, the resultant XPS spectrum shows two peaks with intensity ratio 2:1, as can be observed for the pure polymer data in figure 6(b). For the nanocomposite materials the said ratio is found to be altered. For both samples the intensity corresponding to the pendant carbon is reduced compared to the backbone ones. In sample I, where the silver volume fraction is high, this effect is more pronounced, resulting in a ratio 3:1. The reduction in the ratio, as discussed above for the reduction of the O 1s and N 1s peak intensities, may be interpreted in terms of the

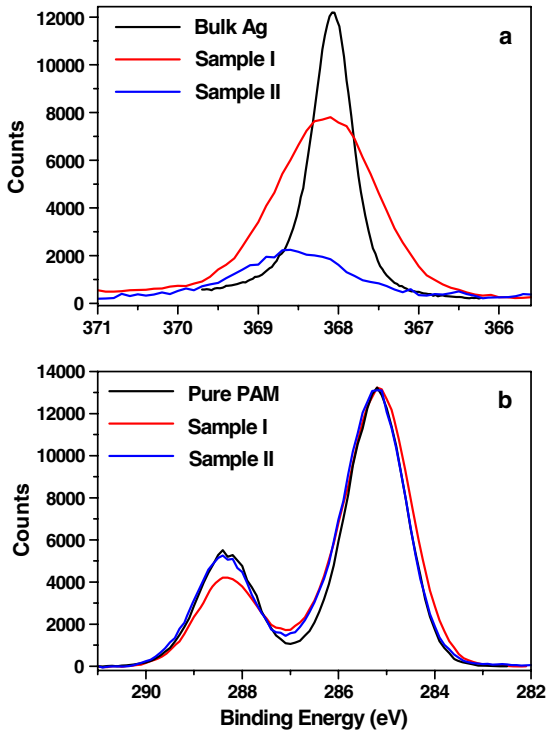

Figure 6. Core level XPS spectra for the different samples. (a) Ag $3d_{5/2}$ spectra for the nanocomposite materials, sample I and sample II, compared with that for bulk Ag; (b) C 1s spectra of pure polymer and nanocomposites. All peak positions were normalized with respect to the major peak in the C 1s spectra at 285.2 eV.

shadowing of the pendant groups, which are directly attached to the particles, by the backbone polymer chains.

In figure 7(a) we have compared the valence band spectra of the two nanocomposite samples with that of the pure PAM. The valence band data provide confirmatory evidence concerning the interacting sites, besides providing information regarding the orbitals that come into play in the interactions. When the valence band data for the pure polymer are suitably subtracted from those of the nanocomposite samples we can clearly see the modifications in the valence bands of silver as well as for the polymer in the composite materials. In figure 7(b) we have shown the silver valence band observed from the two nanocomposite samples along with the same for polycrystalline bulk silver. It has already been shown that the valence band of the nanocrystalline silver particles is likely to be shifted towards higher binding energy along with the reduction of their widths [28], which is also observed in our case. In the present study, the changes observed in the valence band of the nanocrystalline silver are attributed to the quantum size effect of the particles, whereas the valence band of the polymer reflects the effects of polymer–particle interaction. In figure 7(a) the changes in the valence band spectra of the nanocomposite material for the energy range 7–30 eV are shown. There is an observable increase in the widths for the valence band peaks for the nanocomposite materials which indicates larger dispersion in the valence band as a result of polymer–particle interaction. The positions of the O 2s and N 2s peaks at 26.8 and at 22.2 eV respectively for the pure polymer are found to be nearly unaltered [29] for the composites. It is known that the structure

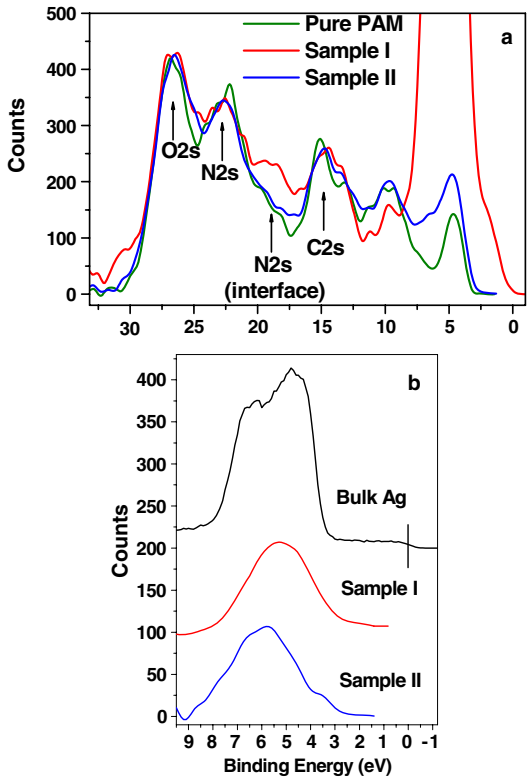

Figure 7. (a) XPS valence band spectra of pure polymer and nanocomposites; (b) valence band of Ag nanoparticles in polyacrylamide support, in comparison to bulk polycrystalline silver. The polymer contribution has been subtracted from each spectrum. The vertical line denotes the position of the Fermi level in bulk Ag. The curves have been scaled and shifted vertically for clarity.

of overlapping peaks arising between 22 and 7 eV is due to additional orbitals formed from the interaction of C 2s/2p, O 2p, N 2p and H 1s orbitals [30]. It is important to note that at the present photon energy the ionization cross sections of the 2p level of carbon is about two orders of magnitude smaller than that of 2s; for oxygen and nitrogen these differences are about one order of magnitude [31]. Thus it is unlikely that we see any 2p levels in the valence band spectra. We therefore assign the large peak close to 15 eV to the 2s level of carbon. The only prominent change in the valence band of the nanocomposite compared to that of pure PAM is the appearance of a new peak around 19 eV. It has been observed that the metal surface plays the role of electron donor in the case of polymer–metal interaction [27, 32]. We believe that the additional peak at 19 eV appears from the N 2s excitations of the nitrogen molecules that are attached to the surface of the silver particles. The shift to lower binding energy of the N 2s peak may be attributed to the partial electron transfer from the metal surface to the attached nitrogen atoms in support of our observation that the reduction process of silver metals slows down in the presence of the polymer. The peak is less prominent for sample II, where the surface component is less due to lower volume fraction of silver in this sample. Since there is no change in the core level of the N 1s line, we consider the interaction to be physical or weakly chemical in nature. There are reports in the literature that nitrogen plays a dominant role compared to oxygen in case of polymer–metal interaction for oxygen- and nitrogen-containing polymers [27]. Here also the primary interaction between the silver

nanoparticles and the polymer molecules occurs through the nitrogen sites and as the bond strength of C=O (798.9 kJ mol^{-1}) is much higher than that for C–N (304.6 kJ mol^{-1}) [33], the role of oxygen in the interaction with the nanoparticles is somewhat secondary.

4. Conclusion

We have prepared silver–polyacrylamide nanocomposite materials with two different metallic volume fractions through a chemical route and used spectroscopic techniques to study the interactions between the polymer and the metallic nanoclusters. Larger spectral modifications, compared to the pure polymer, are seen for the composite containing a higher volume fraction of silver, and are indicative of the fact that the polymer molecules attached to the metal surface are mainly affected by the polymer–metal interaction. The DLS and TEM observations indicate that in the nanocomposite material the silver nanoparticles are encapsulated by the polymer chains. Optical absorption data for the nanocomposite also confirms the presence of agglomerated polymer-coated silver nanoclusters. The modification of the FTIR spectra for the nanocomposite materials indicates that the nanocrystalline particles are directly attached to the polymer chains through attractive interactions at the pendant parts of the chains. The XPS spectra for silver indicate the confinement effect of the non-interacting nanoparticles. The reduction of intensities of O 1s and N 1s lines points to the fact that these atoms are more populated at the polymer–metal interface. The analysis of the valence band spectra of the polymeric atoms confirms that the nitrogen sites in this polymer act as partial electron acceptors from the metallic nanoparticles and thereby create an attractive physical or weak chemical interaction leading to the adsorption of the metal particles specific to the nitrogen sites in the pendant part of the polymer molecules.

Acknowledgment

The authors gratefully acknowledge Supriyo Chakraborty for his contributions in the TEM measurements.

References

[1] Halperin W P 1986 *Rev. Mod. Phys.* **58** 533
[2] Mishra L C (ed) 2003 *Scientific Basis for Ayurvedic Therapies* (Boca Raton, FL: CRC Press)
[3] Cupp M J and Tracy T S (ed) 2003 *Dietary Supplements: Toxicology and Clinical Pharmacology* (New Jersey: Humana Press)
[4] Zand J, Spreen A N and LaValle J B 1999 *Smart Medicine for Healthier Living* (New York: Avery)
[5] Sun Y and Xia Y 2002 *Science* **298** 2176
[6] Zhu Y, Qian Y, Lic X and Zhang M 1997 *Chem. Commun.* 1081
[7] Yin Y, Xu X, Ge X and Zhang Z 1998 *Radiat. Phys. Chem.* **53** 567
[8] Quaroni L and Chumanov G 1999 *J. Am. Chem. Soc.* **121** 10642
[9] Bonet F, Tekaia-Elhsissen K and Sarathy K V 2000 *Bull. Mater. Sci.* **23** 165
[10] Rogach A L, Shevchenko G P, Afanas'eva Z M and Sviridov V V 1997 *J. Phys. Chem.* B **101** 8129
[11] Mukherjee M, Chakravorty D and Nambissan P M G 1998 *Phys. Rev.* B **57** 848
[12] Singh A and Mukherjee M 2005 *Macromolecules* **38** 8795
[13] Singh A and Mukherjee M 2004 *Phys. Rev.* E **70** 051608
[14] Wang C, Stewart R J and Kopecek J 1999 *Nature* **397** 417
[15] Kopecek J, Kopeckova P, Minko T, Lu Z R and Peterson C M 2001 *J. Control. Release* **74** 147
[16] Rivas B L, Pereira E D and Moreno-Villoslada I 2003 *Prog. Polym. Sci.* **28** 173
[17] Mukherjee M, Saha S K and Chakravorty D 1993 *Appl. Phys. Lett.* **63** 42
[18] Kreibig U 1974 *J. Phys. F: Met. Phys.* **4** 999

[19] Papavassiliou G C 1979 *Prog. Solid State Chem.* **12** 185
[20] Hövel H, Fritz S, Hilger A, Kreibig U and Vollmer M 1993 *Phys. Rev.* B **48** 18178
[21] Persson B N J and Liebsch A 1982 *Solid State Commun.* **44** 1637
[22] Kreibig U and Genzel L 1985 *Surf. Sci.* **156** 678
[23] Quinten M and Kreibig U 1986 *Surf. Sci.* **172** 557
[24] Silverstein R M and Webster F X 1998 *Spectrometric Identification of Organic Compounds* 6th edn (New York: Wiley)
[25] Zhu J F and Zhu Y J 2006 *J. Phys. Chem.* B **110** 8593
[26] Shirley D A 1972 *Phys. Rev.* B **5** 4709
[27] Qiu L, Liu F, Zhao L, Yang W and Yao J 2006 *Langmuir* **22** 4480
[28] Paszti Z, Petö G, Horvath Z E, Karacs A and Guczi L 1998 *Solid State Commun.* **107** 329
[29] Beamson G and Briggs D (ed) 2000 *The XPS of Polymers Database* (Manchester: Surface Spectra Ltd)
[30] Briggs D 1998 *Surface Analysis of Polymers by XPS and Static SIMS* (Cambridge: Cambridge University Press)
[31] Yeh J-J 1993 *Atomic Calculation of Photoionization Cross-Sections and Asymmetry Parameters* (USA: Gordon and Breach Science)
[32] Kim D H and Jo W H 2000 *Macromolecules* **33** 3050
[33] Huheey J E, Keiter E A and Keiter R L 2000 *Inorganic Chemistry: Principles of Structure and Reactivity* (New York: Harper Collins)